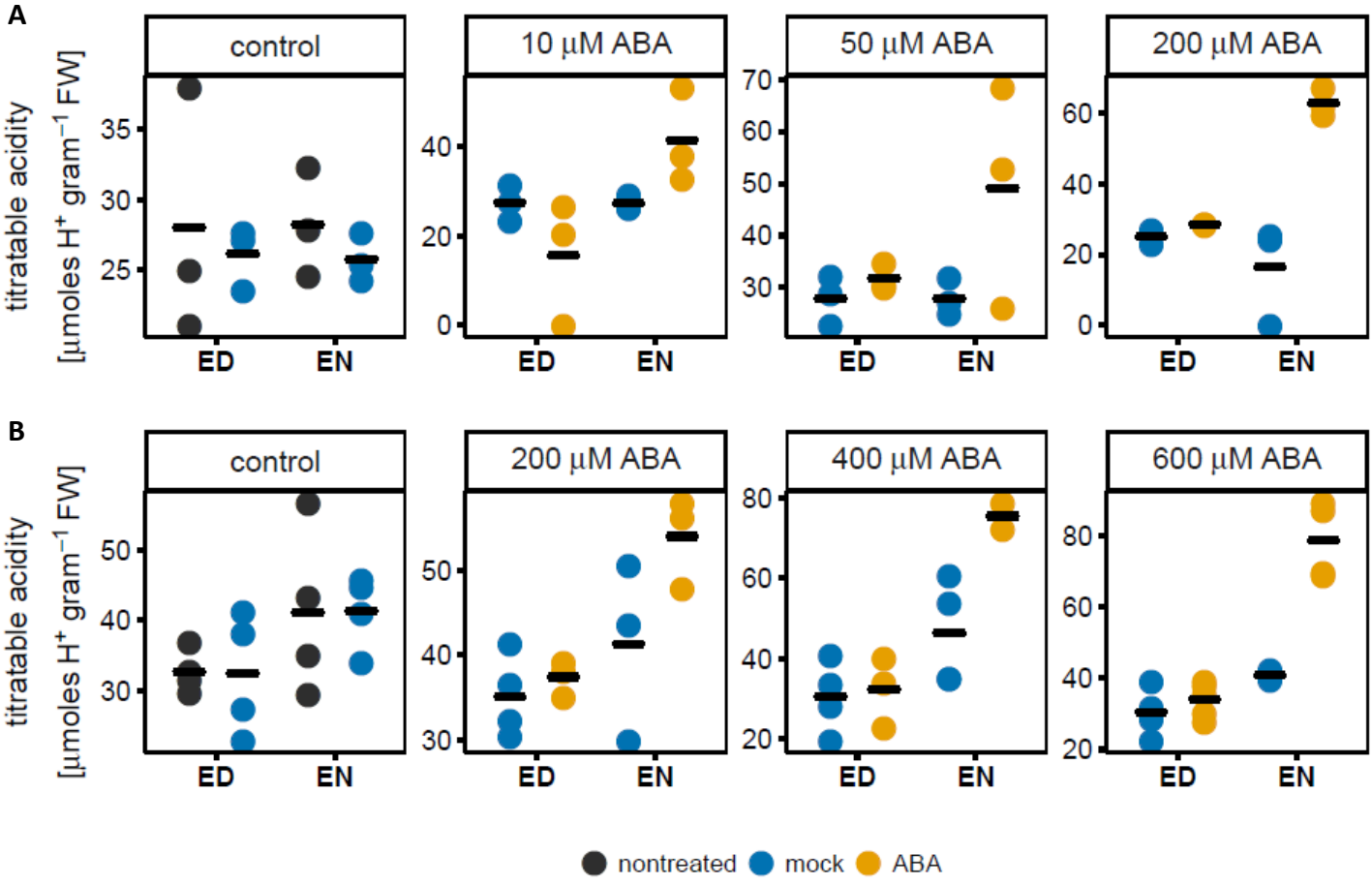

Figure S1. End of day (ED) and end of night (EN) titratable acidity in mature leaves of *Talinum triangulare;* two independent treatments, (A) and (B), with ABA solutions of the given concentration or mock solution (1.86% (v/v) methanol, 0.02% (v/v) Tween-20) applied as foliar spray within the first hour of the light. Plants were grown in 12/12 L/D regime. Paired leaves were treated with mock or ABA solution, nontreated controls were included as well. Leaves were harvested and shock frozen after daily treatments for five consecutive days. Approximately 0.5 g leaf material (fresh weight) was boiled in 40 ml 50% (v/v) methanol until the volume halved. Upon refilling to 40 ml with water, leaves were boiled further until the volume halved again. Finally, extract volume was refilled back to 40 ml one final time with water. After cooling to room temperature, obtained extracts were titrated with 5mM KOH to pH = 7.0, using a pH meter to monitor the change in pH.

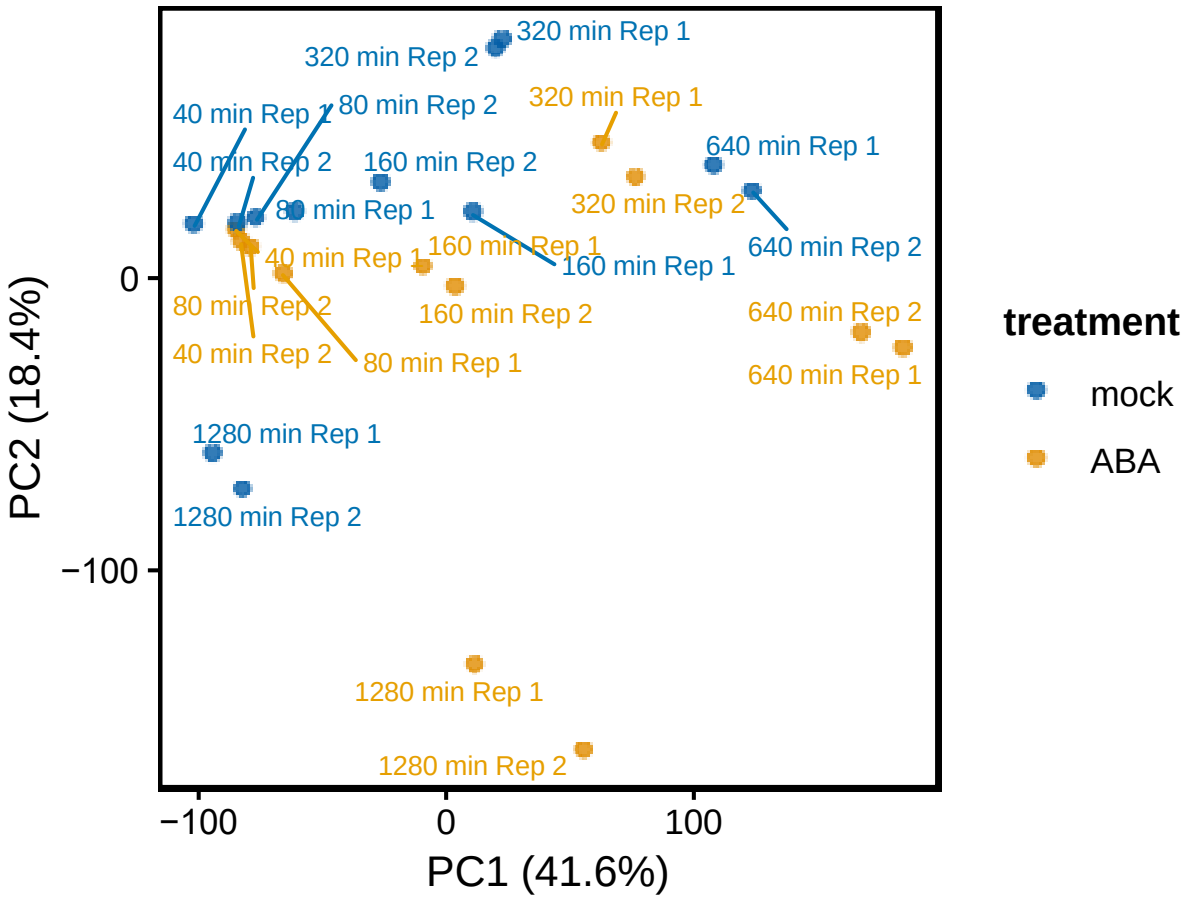

Figure S2. Principle component analysis of RNA-seq data for mock- (blue) and ABA-treated (orange) leaves of *Talinum triangulare* harvested 40, 80, 160, 320, 640 and 1280 min after the first ABA treatment.

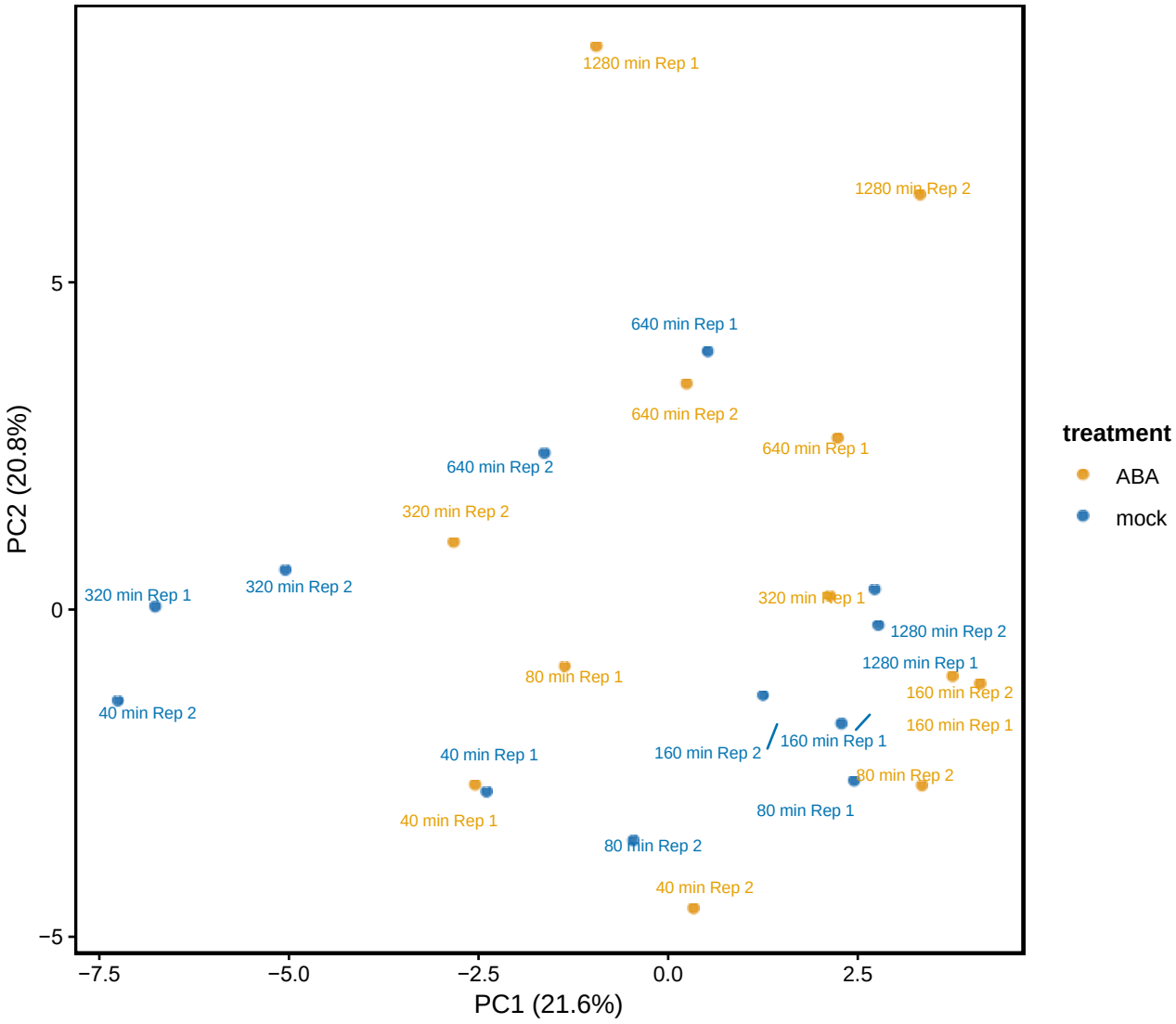

Figure S3. Principle component analysis of metabolite amounts detected in leaves of *Talinum triangulare* harvested 40, 80, 160, 320, 640 and 1280 min after the first ABA treatment (mock in blue and ABA in orange). The shown PCA is based on metabolite amounts measured with GC-MS and LC-MS.

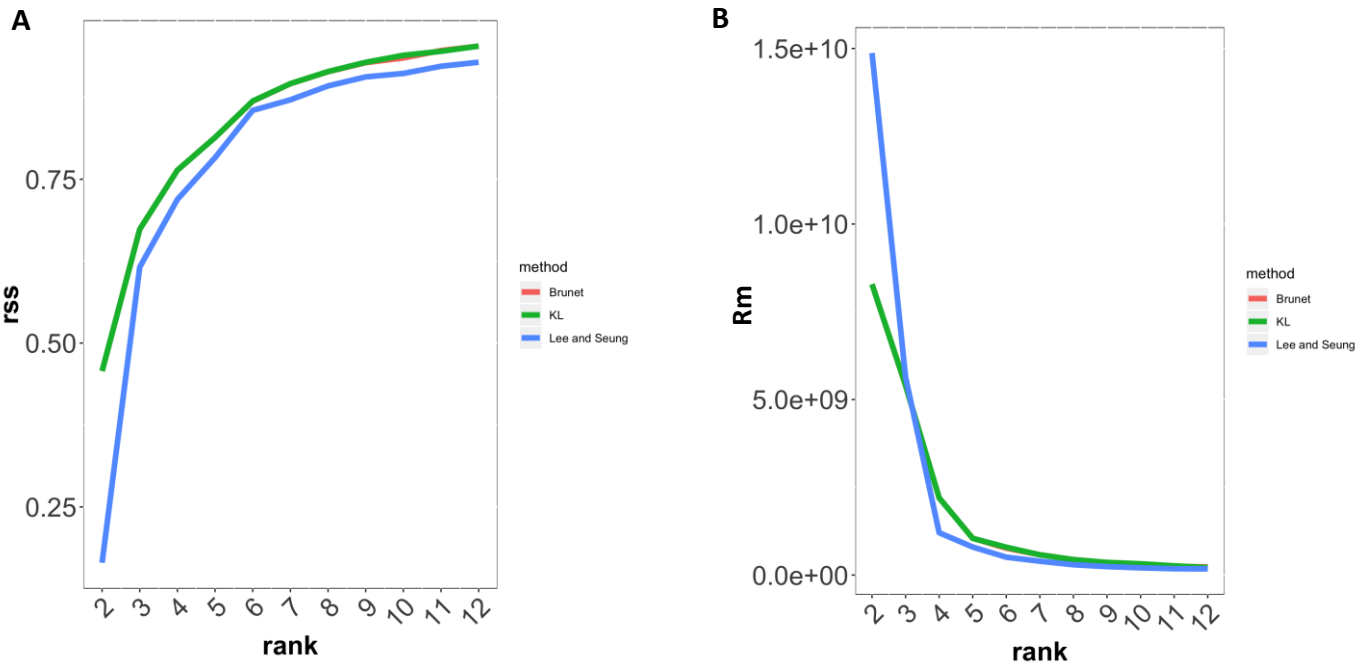

Figure S4. Comparison of performance of Lee and Seung (blue), Brunet (red), and KL (green) algorithms in terms of (A) residual sum of squares and (B) average regression coefficient (R^2). The algorithms were tested prior to running nonnegative matrix factorization (NMF) on the transcriptome data set obtained for *Talinum triangulare*. All three algorithms identified five factors.

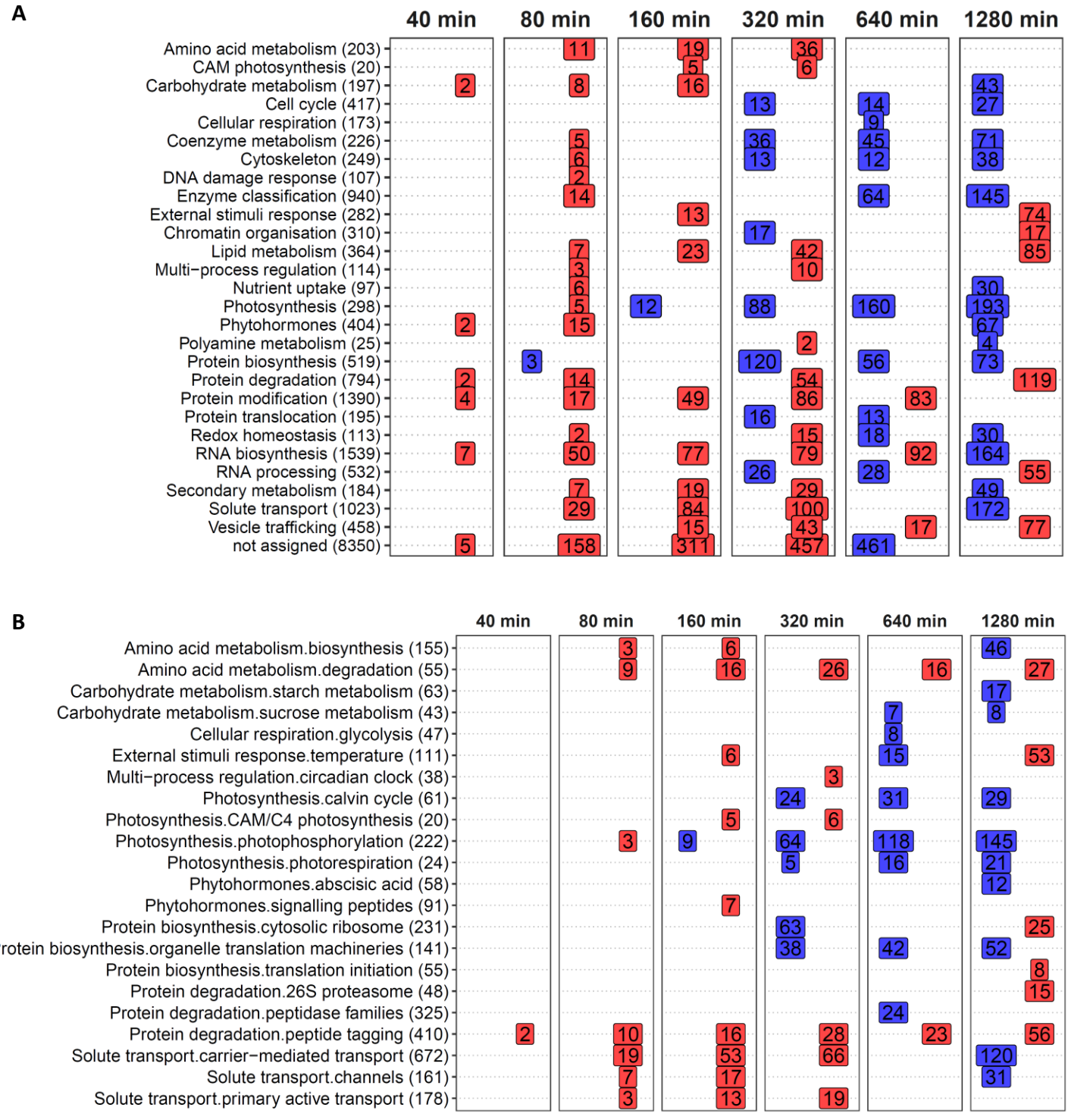

Figure S5. Over-representation of biological functions at individual sampling time points. (A) MapMan categories in the first bin. (B) Selected MapMan categories at the level of second bin. *Talinum triangulare* reads were mapped against *Beta vulgaris* reference and after mapping, only transcripts with a known homolog in Arabidopsis were used in the enrichment analysis. Up- and down-regulation of individual transcripts was based on DESeq analysis (q-value ≤ 0.01 after false discovery rate correction according to Benjamini & Hochberg). Enrichments are based on Wilcoxon test with false discovery rate correction according to Benjamini & Hochberg and significance level of 0.05. When multiple *Beta vulgaris* targets mapped against a single Arabidopsis gene, all hits were counted. Numbers in brackets stand for total number of mapped genes in each category. In red is number of up-regulated and in blue number of down-regulated genes The complete list of gene assignments to MapMan bins, incuding manually expanded CAM/C_4 photosynthesis, is available as Supplemental Table 2.

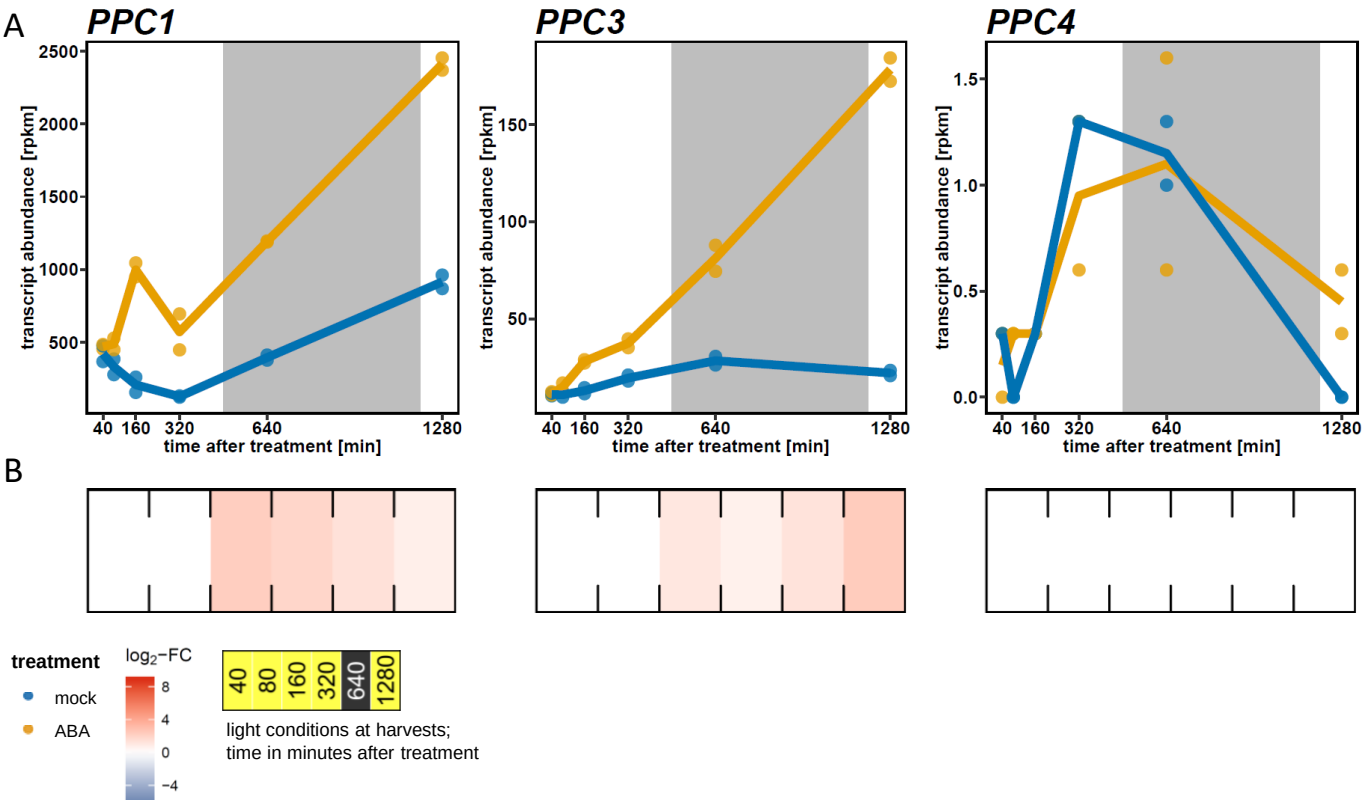

Figure S6. Transcript abundance of three detected isoforms of *PPC* in *Talinum triangulare* leaves. (A) Absolute transcript levels [rpkm]. (B) Differential expression in ABA-treated compared to mock-treated leaves (DESeq analysis). In the DESeq analysis, only significantly different (*q*-value ≤ 0.01) changes are shown.

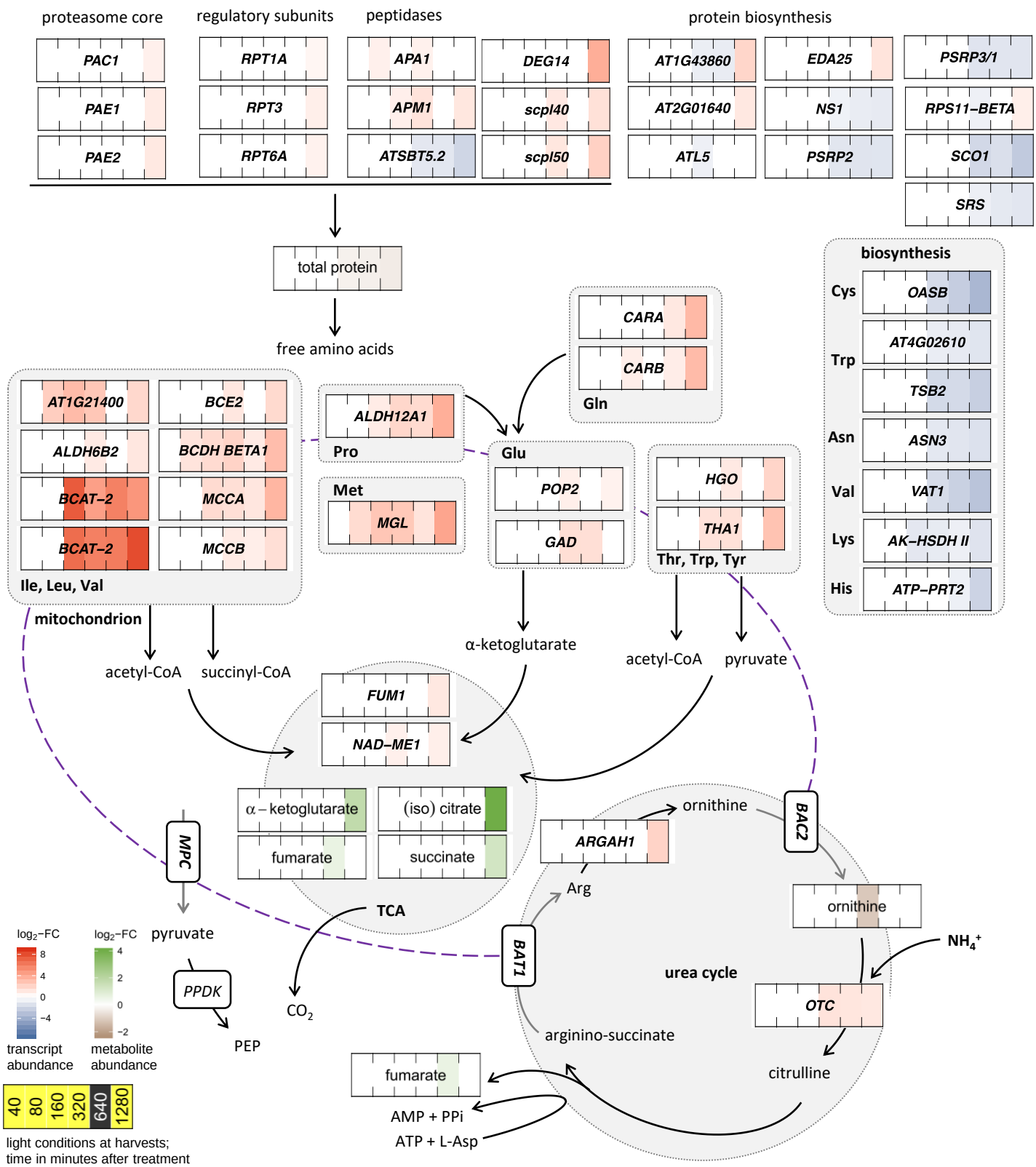

Figure S7. ABA-induced changes in abundances of transcripts encoding components of protein degradation/synthesis and amino acid degradation/synthesis pathways in *Talinum triangulare*. Transcript abundances are expressed as $\log_2$-fold changes of ABA- compared to mock-treated leaves (n = 2). Only genes with significantly different transcript abundance (DESeq with Benjamini & Hochberg correction, *q*-value < 0.01) and altered temporal pattern (maSigPro with Benjamini & Hochberg correction, *q*-value < 0.01 and $R^2 > 0.8$) are shown. In response to ABA, primarily protein and amino acid degradation pathways are up-regulated, with up-regulation of amino acid-degrading enzymes preceeding that of enzymes of protein degradation. Degraded amino acids provide carbon backbones in the form of pyruvate or TCA intermediates. Pyruvate could be subsequently phosphorylated by PPDK to produce PEP, a substrate for nocturnal carbon assimilation. Generated organic acids can enter the TCA cycle and thus support energy production required *e.g.* to fuel synthesis and transmembrane transport processes. Additionally, CO_2 originating both from respiration and amino acid degradation could be potentially captured by PPC besides ambient CO_2. MPC, mitochondrial pyruvate carrier; OAA, oxaloacetate; PEP, phospho*enol*pyruvate; TCA, tricarboxylic acid cycle.

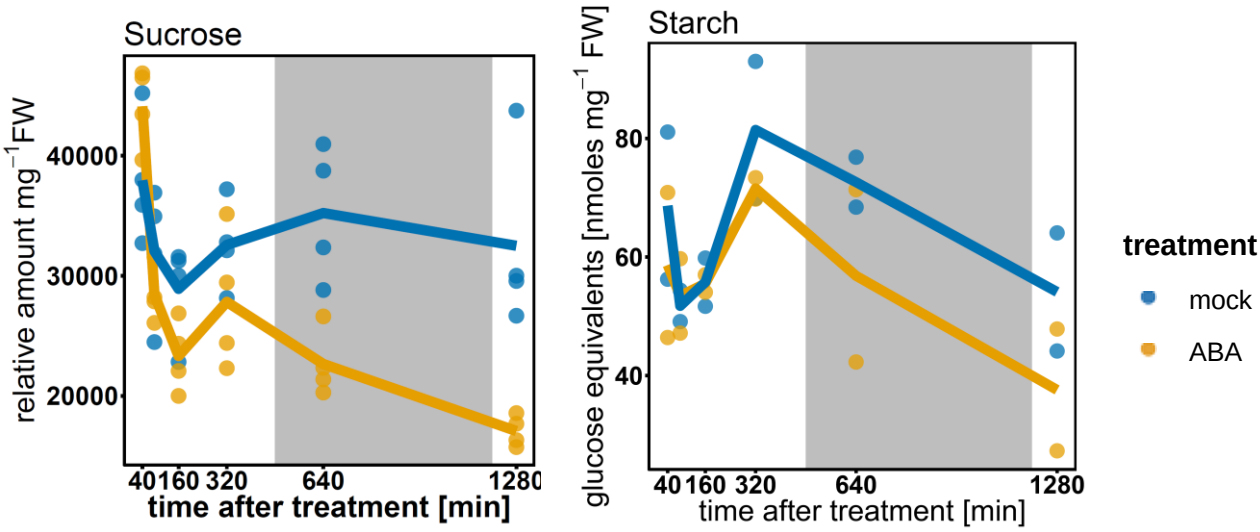

Figure S8. Diurnal pattern of sucrose and starch abundances in mock- (blue) and ABA-treated (orange) leaves of *Talinum triangulare*. While the observed changes are not significant (q-value ≤ 0.05), there seems to be a trend towards nocturnal depletion of both carbon sources already during the first dark period after the ABA treatment.